Silicon-on-insulator structures microtopography transformations features after photonic and corpuscular radiation exposure

© B.A. Loginov,[1] D.Yu. Blinnikov,[2] V.S. Vtorova,[2] V.V. Kirillova,[2] E.A. Liashko,[2] V.S. Makeev,[2] A.R. Pervykh,[2] N.D. Abrosimova,[3] I.Yu. Zabavichev,[3,4] A.S. Puzanov,[3,4] E.V. Volkova,[4] E.A. Tarasova,[4] S.V. Obolensky[3,4]

[1] National Research University of Electronic Technology (MIET),
124498 Zelenograd, Russia
[2] Educational Center „Sirius“,
354349 Sochi, Russia
[3] Federal State Unitary Enterprise RFNC-VNIIEF,
RFNC-VNIIEF Branch „Measuring Systems Research Institute named after Yu.Ye. Sedakov“,
603950 Nizhny Novgorod, Russia
[4] Lobachevsky University of Nizhny Novgorod,
603600 Nizhny Novgorod, Russia
e-mail: andnenastik@inbox.ru

The article presents the results of studies of microrelief parameters and electrophysical characteristics of „silicon on insulator“ structures after exposure to gamma and gamma neutron radiation. Experimental studies were carried out using the methods of atomic force microscopy and pseudo-MOS transistor. On the basis of the data obtained, an estimate was made of the average size and area of the space charge of clusters of radiation defects.

Keywords: AFM, silicon on insulator, pseudo-MOS, „subthreshold“ defect formation, radiation defects clusters.

Introduction

Surface microgeometry is one of the most sensitive characteristics of semiconductor materials when exposed to ionizing radiation. Especially the importance of surface quality increases in the light of the miniaturization of modern electronic components. Understanding the mechanisms of surface rearrangement under destabilizing influences is important for predicting the response of nanoelectronic devices to radiation exposure.

1. Objects of study

The objects of study were „silicon-on-insulator“ structures produced using hydrogen transfer technology. The device layer and the substrate had p-type of conductivity and crystallographic orientation $\langle 100 \rangle$. The thicknesses of the device layer and the hidden dielectric were 200 nm. The electrophysical characteristics and microrelief parameters of structures irradiated with gamma radiation were compared with the characteristics of structures exposed to gamma neutron radiation and compared with the characteristics of control samples. The reference samples are designated as 5N. Samples exposed to gamma radiation are designated as 5U. Samples exposed to gamma-neutron radiation are designated as 5R.

2. Experiment procedure

„Scanning probe microscope SMM-2000“ [1] manufactured by PROTON factory, Zelenograd, certificate RU.C.27.004.A №.42785 on entry into the State Register of Measuring Instruments of the Russian Federation was used to study the microrelief. The samples were examined without any additional processing, in the mode of atomic-force microscopy (AFM), while super-sharp cantilevers „MSNL“ from Brucker, USA, with a radius of rounded tip 2 nm were used as probes.

The average area of clusters formed after radiation exposure [2,3] was estimated.

Measurements by the pseudo-TIR transistor [4] were carried out using a system for measuring electrophysical parameters with a mercury probe.

3. Results and discussion

The nature of the microrelief, as can be seen from Fig. 1, is markedly different on all types of samples studied. The main results of statistical image processing are summarized in Table 1. It can be seen that larger-scale structures are formed in case of a gamma-neutron irradiation, than in case of a gamma radiation, which is associated with a higher average initial energy of primary knocked-on atoms when exposed to corpuscular radiation compared to photonic of the same energies. The exception is the average
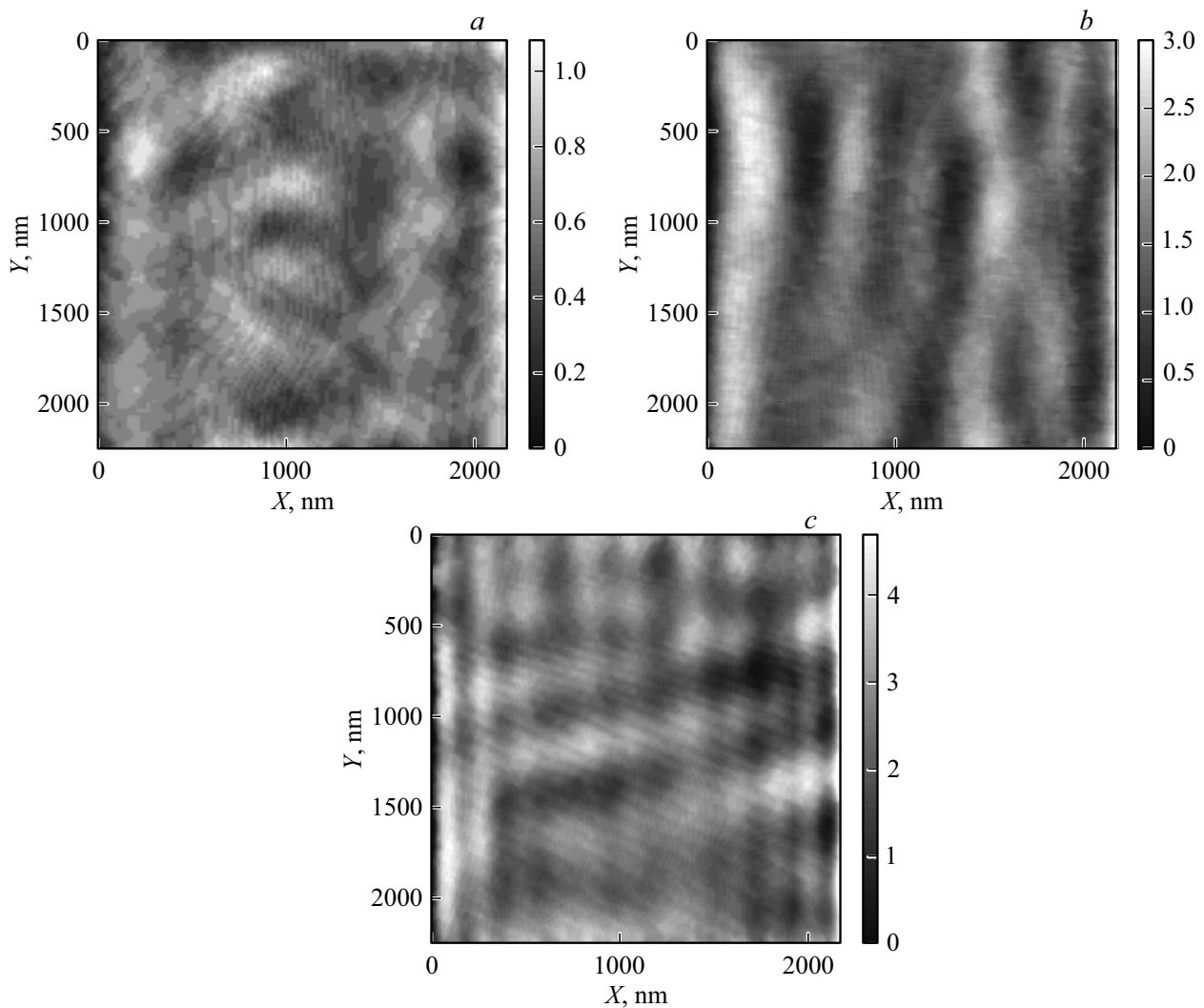
Figure 1. Microrelief of the surface of the samples: a — 5N, b — 5R, c — 5U, the frame size for the sample is 5N — 2.16 μm (X)/2.25 $(Y)\,\mu$m, for samples 5R, 5U — 2.17 μm (X)/2.26 $(Y)\,\mu$m.

Table 1. Statistical characteristics of the sample surface before and after exposure to radiation

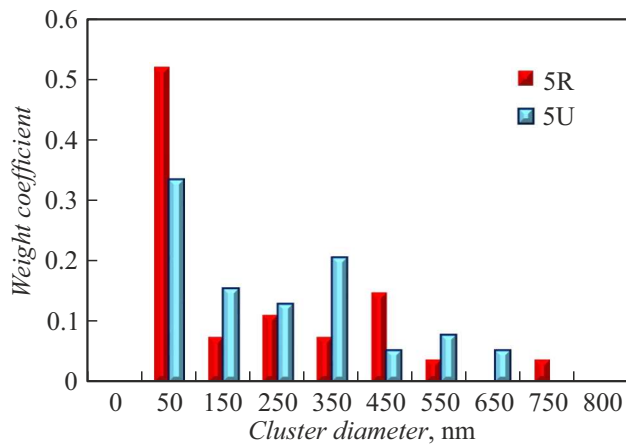| Parameter	Sample		
	5N	5U	5R
Root-mean-square roughness, pm	100.4	219.4	391.3
Average roughness, pm	81.85	187.1	318.7
Roughness by 10 points, pm	257.8	609.8	759.4
Maximum development of the relief, pm	514.0	839.1	1950.0
Average distance between peaks of the relief profile, nm	267.7	296.5	439.1
Average distance between profile minima, nm	139.1	76.71	63.07
The root-mean-square slope of objects, °	0.121	0.254	0.367
Average slope of objects, °	0.085	0.192	0.268

Figure 2. Diagram of average cluster sizes in samples after gamma and gamma neutron exposure.

distance between the minima of the relief profile, reflecting, apparently, a more developed structure of subclusters of radiation defects formed when exposed to gamma radiation.

To find the size distribution of the nuclei of clusters of radiation defects formed after gamma and neutron effects, the following processing algorithm was used:

— preliminary median AFM image filtering to eliminate pulse interference;

— opening operation with subtraction of smoothly changing background and highlighting of identified areas by linear contrast;

— automatic search for linked areas with counting the number of pixels n_i in each object;

— calculation of the areas S_i of linked areas, where i is the ordinal number of the area, according to the formula $S_i = n_i \times \Delta x \times \Delta y$. Here $\Delta x \approx 3.11$ nm and $\Delta y \approx 3.24$ nm are the linear pixel dimensions of the AFM image;

— calculation of the effective radius of clusters using the formula $r_i = \sqrt{\frac{S_i}{\pi}}$.

It should be noted that it is possible to define clusters with an effective radius of at least 5.37 nm using this technique because the minimum filter size is 3×3 pixels.

Analyzing the distribution of clusters of radiation defects shown in Fig. 2, it can be concluded that larger clusters occur in case of a neutron exposure, but the cluster density is higher in case of a gamma radiation exposure, which also directly follows from the data given in Table. 1.

A qualitative analysis of the electronic component of the pseudo-MDT volt-ampere curve shown in Fig. 3 shows that, firstly, the magnitude of the drain current after irradiation decreased by two orders of magnitude, and secondly, the value of volumetric leaks and hole mobility decreased. The built-in charge, as can be seen from Table 2, has changed the sign. The value of the built-in charge and mobility is slightly higher for structures exposed to gamma-neutron radiation. It should also be noted a smoother type of volt-ampere characteristic for the case of exposure to gamma radiation.

Table 2. Values of electrophysical characteristics of „silicon-on-insulator" structures after gamma and gamma neutron radiation

t days	0	20		27		34	
Type of exposure	N	U	R	U	R	U	R
μ_p, cm^2/(V·s)	250	34	30	50	70	60	90
Q_{tot}, 10^{10} cm^{-2}	-5	8	6	7	4	7	3
D_{it}, 10^{11} eV^{-1}·cm^{-2}	**3,2**	**2**	**2**	2	2	2	2

Note: μ_p — mobility of holes in the instrument layer, Q_{tot} — fixed charge in the buried dielectric, D_{it} — density of surface states at the boundary of the buried dielectric and the instrument silicon layer.
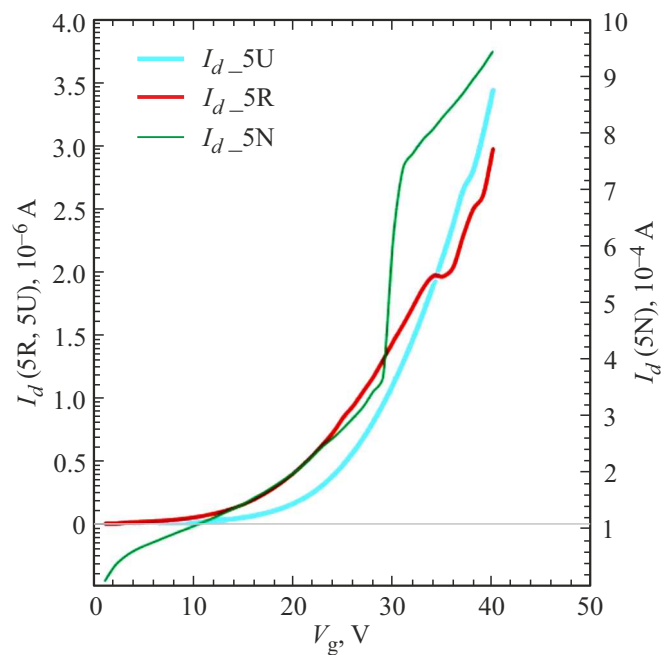

Figure 3. Volt-ampere curve of samples of type 5N, 5R, 5U obtained using the pseudo-MDT transistor method (electronic component).

Changes in the slope in the voltage range of more than 30 V are observed on the volt-ampere curve after exposure to gamma-neutron radiation.

Clusters of radiation defects formed as a result of migration of primary defects may have a conductivity different from that of the main volume of the material. The magnitude of the potential barrier resulting from the depletion of the spatial charge region by free carriers due to the capture of charge at deep energy levels of defects in the disordered region is determined by the size and degree of the damage zone and the concentration of electrically active impurities in it. Thus, the probability of capturing non-core carriers increases, and the probability of capturing main carriers decreases. The size of the depletion regions of clusters ranges from 5 to 50 nm, they are enriched with vacancies and their associations such as divacancies,

trivacancies, etc. Being centers of scattering and capture of carriers, disordered regions have a significant impact on the electrophysical characteristics of semiconductor materials. The size of the cluster, rather than the density of their location, has a more noticeable effect on the electrophysical characteristics according to the data given in Table. 2 and in Figs. 2 and 3.

The data listed in Table 2 show that the density of surface states and the mobility of holes after a long time after radiation exposure do not differ for gamma and gamma neutron exposure. The differences in the response to radiation exposure are significant for the mobility of electrons.

One of the possible mechanisms of transformation of the microrelief in case of the radiation exposure is the process of defect formation, in which point defects are formed in a solid. The interaction of primary point defects formed in case of the radiation exposure with the initial defects of the semiconductor structure (pore boundaries, dislocations, etc.) is the cause of the formation of secondary radiation defects, including stable complexes of disordered regions, called clusters formed by one or more cascades of atomic collisions. The cluster has a branched structure of primary and secondary displaced atoms. A subcluster is formed at the point of stopping of the displaced atoms. The set of subclusters, branches and isolated defects will be called a supercluster. The size of the supercluster can reach fractions of a micron.

At present, there is a wide range of methods for modeling the development of cascades of atomic collisions in matter [5], which can be divided into 4 classes: quantum-mechanical methods„from first principles", methods of classical molecular dynamics, stochastic methods (Monte Carlo algorithms) and continuum methods based on the laws of heat-and-mass transfer in continuous medium. The presented algorithms have different computational complexity, which is determined by the spatial and temporal resolution while maintaining the required accuracy of the solution.

The basis of quantum mechanical methods „from the first principles" is the determination of the trajectories of the nuclei of the crystal lattice and electrons based on the solution of the multiparticle nonstationary Schrödinger equation. The movement of electrons is considered as the movement of independent particles in the potential created by other electrons and atomic nuclei to simplify the problem. However, due to computational complexity, the method is limited to systems consisting of several hundred atoms whose dynamics are modeled over several femtoseconds [6]. Therefore, at present, the quantum mechanical method is not used in practice to simulate the development of cascades of atomic collisions in matter.

Following the path of simplification of the task, it is possible to consider the electronic and atomic subsystem separately from each other. In this case, it is possible to abandon the quantum-mechanical description of the development of the cascade of atomic collisions, replacing the Schrödinger equation with the laws of classical mechanics. The molecular dynamics method is based on the use of Newton's II law for each atom of the system.

The spatial and temporal limitations of the molecular dynamics method are due to the same reasons as those of quantum mechanical methods, and allow simulating the formation of clusters of radiation defects in volumetric regions with a linear size in each of the coordinates up to hundreds of nanometers for several hundred picoseconds [7]. The time integration step should correspond to the dynamics of the ongoing processes and can be changed during the simulation procedure to increase the efficiency of calculations.

I is necessary to switch from a deterministic approach to describe the ongoing phenomena to a stochastic one to further increase the spatial and temporal scales of modeling the process of formation of a disordered region of radiation defects.

In Monte Carlo simulation, the trajectory of each atom begins with the introduction of its position, direction of motion and energy [8,9]. Then the sequence of collisions with the atoms of matter is traced, and between collisions the free path of the atom is assumed to be rectilinear. The energy of the particle decreases on each free path by the amount of electronic energy losses, and then after the collision it decreases by the amount of nuclear or elastic energy losses, i.e. by the amount of energy transferred to the target atom in case of the collision. If an atom of a substance receives energy that exceeds a predetermined value, then it is called a secondary knocked-on atom and its behavior is traced in the same way as the behavior of the intruder. The same remains true for any following knocked-on atoms. The trajectory of the knocked-on atom ends if its energy decreases to a preset value.

Continuous methods are used to model the processes of annealing radiation defects on large spatial and temporal scales. In this case, a greater spatial and temporal resolution is achieved due to the transition from the consideration of individual atoms (both moving and bound into a crystal lattice) of the studied material to a continuous (solid) medium, to an infinitesimal volume of which certain values of thermodynamic variables can be attributed.

The analysis of the presented methods shows that at present quantum mechanical methods are practically inapplicable for modeling the development of cascades of atomic collisions in matter, due to the extremely high computational complexity. Thus, the combination of classical molecular dynamics methods (for dense clusters of radiation defects) and Monte Carlo (for sparse clusters of radiation defects) at the stage of formation of the displacement cascade ($t < 10^{-12}$ s) with heat and mass transfer methods at the stage of rapid annealing of radiation defects ($t < 10^{-9}$ s). In the following part of the work, the application of the classical molecular dynamics method for modeling the formation of a cascade of atomic displacements near the surface of a semiconductor under the action of a stream of

instantaneous neutrons of the fission spectrum is considered in detail.

Numerical simulation was performed to estimate the parameters of clusters of radiation defects arising on the surface of the irradiated structure using the molecular dynamics method implemented in the LAMMPS [10] application software package. The size of the calculated region was $500 \times 500 \times 500$ Å (~ 8000000 atoms), in which the evolution of a disordered region of atomic displacements over 100 ps formed by a primary silicon knocked-on atom with different kinetic energy was modeled. A method based on the construction of Wigner-Seitz cells was used to determine the location of defects in the simulated system. The Stillinger-Weber potential was chosen as the interatomic interaction potential [11]:

$$U(r) = \sum_i \sum_{j>i} U_2(r_{ij}) + \sum_i \sum_{j \neq i} \sum_{k \neq j \neq i} U_3(r_{ij}, r_{ik}, \Theta_{ijk}),$$

$$U_2(r_{ij}) =$$

$$= \begin{cases} A_{ij}\varepsilon_{ij}\left[B_{ij}\left(\frac{\sigma_{ij}}{r_{ij}}\right)^{p^{ij}} - \left(\frac{\sigma_{ij}}{r_{ij}}\right)^{q^{ij}}\right]\exp\left(\frac{\sigma_{ij}}{r_{ij}-a_{ij}\sigma_{ij}}\right), & r_{ij} \leq a_{ij}\sigma_{ij} \\ 0, & r_{ij} \geq a_{ij}\sigma_{ij}, \end{cases}$$

$$(1)$$

$$U_3(r_{ij}, r_{ik}, \Theta_{ijk}) = \lambda_{ijk}\varepsilon_{ijk}\left[\cos(\Theta_{ijk}) + \cos(\Theta_{0ijk})\right]^2$$

$$\times \exp\left(\frac{\gamma_{ij}\sigma_{ij}}{r_{ij}-a_{ij}\sigma_{ij}}\right)\exp\left(\frac{\gamma_{ik}\sigma_{ik}}{r_{ik}-a_{ik}\sigma_{ik}}\right),$$

where A, B, p, q, a, λ and γ — dimensionless model parameters; a σ — cutoff distance, ε — the dimensional coefficient. This potential is used because the data obtained using it are in good agreement with the theoretical results of modeling and experiment [12].

A two-temperature model jcite13 was used to account for the electronic losses of moving atoms, which is based on the thermal diffusion equation

$$C_e\rho_e\frac{\partial T_e}{\partial t} = \nabla(K_e\nabla T_e)\cdot - g_p \cdot (T_e - T_a) + g_s T_a, \quad (2)$$

where C_e — the heat capacity of the electron gas, ρ_e — the electron density, K_e — electron conductivity, g_p — electron-phonon interaction coefficient, g_s — electron loss coefficient, T_a and T_e — temperatures of the atomic and electronic subsystem, respectively. It is possible to calculate the energy exchange between atomic and electronic subsystems by solving equation (2) with respect to T_a and T_e.

The previously considered approach was used to simulate the formation of a cluster of radiation defects in the volume of a semiconductor [14]. Two limiting cases of interaction of a neutron with an atom of matter were considered in the course of modeling in this paper. In the first case, a neutron interacts with an atom of the target surface, forming a primary knocked-on atom that moves deep into the sample. Another option is the case when a neutron interacts with an atom in the depth of the target, and as
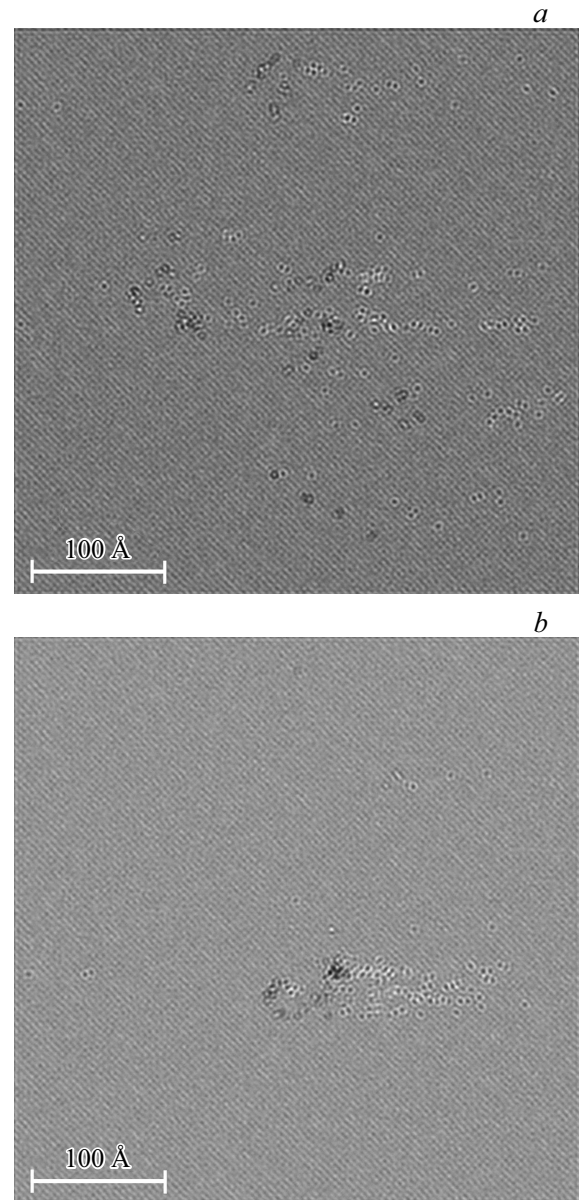

Figure 4. Characteristic images of the target surface for various conditions of formation of clusters of radiation defects: a – the primary knocked-on atom moves from the surface deep into the target; b – the primary knocked-on atom moves from the target towards the surface.

a result of elastic scattering, the primary knocked-on atom moves to the surface of the sample. The energy of the primary knocked-on atom was chosen in accordance with the distribution of fast neutrons of the fission spectrum [15]. Characteristic results of modeling the target surface in the form of images of an electron scanning microscope are shown in Fig. 4.

Two types of structural damage are possible on the surface of a semiconductor material after exposure to a neutron flux according to the results obtained: point defects of the type of Frenkel pairs formed as a result of backscattering of atoms, and clusters of point defects formed

near the departure point of a high-energy knocked-on atom. At the same time, clusters can have different shapes, the lateral dimensions of which can reach tens of nanometers.

When comparing the results of modeling structural damage to the surface under the influence of a fast neutron flux with experimental data, it should be noted that the resolution of the AFM images obtained is insufficient to detect small-scale changes in the relief. Thus, the changes in average roughness observed after radiation exposure are not associated with microstructural damage to the surface. Based on the scale of the observed surface inhomogeneities, their appearance is associated with long-range wave processes that occur when exposed to radiation [16–19].

Conclusion

The results of complex studies of the surface of samples of „silicon-on-insulator" structures exposed to gamma and gamma neutron radiation presented in the paper can be used to analyze the parameters of integrated circuit elements after radiation exposure. Various methods of AFM image analysis: statistical analysis and search for connected regions give consistent quantitative results of the effective sizes of nuclei of clusters of radiation defects under gamma and gamma neutron irradiation. The results obtained are in good agreement with the results of numerical modeling of defect formation on the surface of a semiconductor carried out by the method of classical molecular dynamics. The impact of the size and density of clusters of radiation defects on the mobility of charge carriers has been experimentally confirmed by pseudo-MDT volt-ampere characteristics.

The process of relaxation of structural damage is influenced by clustering mechanisms due to the difference in the nature of gamma and gamma neutron radiation. In composite structures, such as „silicon-on-insulator", the relaxation of electrophysical properties is also further influenced by static and dynamic stresses at the phase interfaces [16]. Relaxation is more likely to have an ionization nature and is attributable to the Coulomb repulsion of ions formed during irradiation in all components of the structures „silicon on the insulator ".

As part of further research, it is planned to conduct an autocorrelation analysis of the AFM images presented and to analyze the impact of changes in micro-roughness on the relaxation time of the charge carrier pulse at the micro level and their mobility at the macro level under various types of radiation exposure.

Funding

Conflict of interest

The authors declare that they have no conflict of interest.

References

[1] B.A. Loginov, P.B. Loginov, V.B. Loginov, A.B. Loginov. Nanoindustry, **12**, 362 (2019).

[2] S.V. Obolensky, E.V. Volkova, A.B. Loginov, B.A. Loginov, E.A. Tarasova, A.S. Puzanov, S.A. Korolev. Pisma v ZhTF, **47** (5), 38 (2021) (in Russian). DOI: 10.21883/PJTF.2021.05.50676.18608

[3] E.V. Volkova, A.B. Loginov, B.A. Loginov, E.A. Tarasova, A.S. Puzanov, S.A. Korolev, E.S. Semenov, S.V. Khazanova, S.V. Obolensky. FTP, **55** (10), 846 (in Russian). DOI: 10.21883/FTP.2021.10.51431.19

[4] D.K. Schroder. *Semiconductor Material and De-vice Characterization* (New Jersey, John Wiley & Sons Inc., 1990)

[5] E.G. Grigoriev, Yu.A. Perlovich, G.I. Soloviev, A.L. Udovsky, V.L. Yakushin. Edited by B.A. Kalin. *Fizicheskoye materialovedeniye. Fizicheskiye osnovy prochnosti. Radiatsionnaya fizika tverdogo tela. Computer modelling* (MEPhI, Moscow, 2008), vol. 4, 696 p.

[6] D.D. Vvedensky. J. Phys.: Condens. Matter., **16**, 1537 (2004).

[7] Y.N. Samolyuk, Y.N. Osetskiy, R.E. Stoller. J. Nucl. Mater., **465**, 83 (2015).

[8] V.S. Vavilov. *Deistvie izluchenij na poluprovodniki* (Fizmatgiz, M., 1963), 264 p.

[9] J.F. Ziegler, J.P. Biersak, U. Littmark. *The Stopping and Range of Ions in Solids* (Pergamon, NY., 1996), 192 p.

[10] S. Plimton. J. Comput. Phys., **117**, 1 (1995).

[11] F.H. Stillinger, T.A. Weber. Phys. Rev. B, **31** (8), 5262 (1985).

[12] A. Jay, M. Raine, N. Richard, N. Mousseau, V. Goiffon, A. Hémeryck, P. Magnan. IEEE Transactions on Nucl. Sci., **64** (1), 141 (2017). DOI: 10.1109/TNS.2016.2628089

[13] D. Duffy, A. Rutherford. J. Phys.: Condens. Matter, **19**, 016207 (2007).

[14] I.Yu. Zabavichev, A.A. Potekhin, A.S. Puzanov, S.V. Obolensky, V.A. Kozlov. FTP, **53** (9), 1279 (2019) (in Russian). DOI: 10.21883/FTP.2019.09.48139.23

[15] E.A. Kramer-Ageev. *Eksperimental'nye metody neitronnykh issledovanij* (Energoizdat, M., 1990)

[16] V.M. Vorotyntsev, V.A. Perevoschikov, V.D. Skupov. *Bazovye protsessy micro- i nanoelektroniki* (Prospekt, M, 2017), 358 p. (in Russian).

[17] P.V. Pavlov, Yu.A. Semin, V.D. Skupov, D.I. Tetelbaum. FTP, **20** (3), 503 (1986) (in Russian).

[18] V.D. Skupov, D.I. Tetelbaum. FTP, **21** (8), 1495 (1987) (in Russian).

[19] Yu.A. Semin, V.D. Skupov, D.I. Tetelbaum. ZhTF, **14** (3), 273 (1988) (in Russian).

Translated by A.Akhtyamov